Size dependences of magnetic properties and switching behavior in FePt $L1_0$ nanoparticles

S. Okamoto,* O. Kitakami, N. Kikuchi, T. Miyazaki, and Y. Shimada
Institute of Multidisciplinary Research for Advanced Materials, Tohoku University, Sendai 980-8577, Japan

Y. K. Takahashi
National Institute for Materials Science, 1-2-1 Sengen, Tsukuba 305-0047, Japan

(Received 26 August 2002; revised manuscript received 18 November 2002; published 26 March 2003)

We have prepared epitaxial FePt $L1_0$ (001) nanoparticles covered with Ag and Pt overlayers and investigated their magnetic behaviors by means of anomalous Hall resistance measurements. The particle shapes are thin oblate spheroids with the aspect ratio (height/diameter) of 1/5. The size is ranging from 1 to 2.5 nm in height and from 5 to 30 nm in diameter. FePt $L1_0$ nanoparticles show extremely large coercivity H_c of about 70 kOe at 10 K, which is close to the anisotropy field H_k of highly ordered FePt $L1_0$. This verifies that the very strong magnetic anisotropy K_u of FePt $L1_0$ remains even in the size of several atomic layers along the *c* axis. For a particle diameter of $D_m < 20$ nm, all the magnetic properties, such as the angular dependence of irreversible switching field, the magnitude of H_c, and their temperature dependence, are fully explained by the coherent rotation model, taking the thermal relaxation into account. Although both Ag- and Pt-coated particles follow the coherent rotation model, the latter always exhibits smaller H_c than the former. Such a decrease in H_c can be explained by assuming an enhancement of the effective magnetic moment caused by ferromagnetic polarization of Pt atoms at the Pt/FePt interface. As the particle size D_m exceeds 20 nm, the magnetic behaviors deviate from the ideal coherent rotation model, suggesting that the magnetization reversal mode changes from coherent to incoherent rotation. The critical diameter $D_m \sim 20$ nm at which the reversal mode changes is in good agreement with the critical diameter predicted by the micromagnetic theory.

DOI: 10.1103/PhysRevB.67.094422 PACS number(s): 75.30.Gw, 75.50.Bb, 75.50.Tt, 75.50.Vv

I. INTRODUCTION

Single-domain nanoparticles are of great interest from the standpoint of high-density magnetic recording technology. In order to attain both high signal-to-noise ratio and thermal stability of the media, noninteracting or very weakly interacting nanoparticles with high magnetic anisotropy energy K_u are indispensable.[1] Equiatomic FePt $L1_0$ particles are the most promising ones, since their K_u of $5-8\times10^7$ erg/cm^3 (Refs. 2 and 3) is one order of magnitude higher than those of the currently used CoCr-based alloys.[4,5] There have been a number of attempts to fabricate granular films and island structures consisting of FePt $L1_0$ particles.[6–10] In spite of these efforts, in most cases, the coercivity H_c of these samples is 10–20 kOe, which is much smaller than the expected anisotropy field H_k of about 100 kOe for single-domain FePt $L1_0$ particles, and, furthermore, little study has been done on the fundamental magnetic properties and switching behavior of FePt $L1_0$ nanoparticles. The reason is that random orientation of the *c*-axis and/or three-variant crystal domains in each FePt $L1_0$ particle is frequently observed and makes the analyses of their magnetic behavior very difficult.[10] In addition to these experimental difficulties, reduction of particle size into the nanoscale region may cause complex magnetic behavior of FePt $L1_0$, because the magnetic anisotropy of FePt $L1_0$ originates from the long-range ordering of alternatively stacked Fe and Pt layers along the *c* axis.[11,12] It is eventually affected by reduction of the dimension along the *c* axis to several atomic layers.[13] Moreover, the surface effect should be also considered for the nanoparticles. The magnetic surface or interface anisotropy, in some cases, is strong enough to alter the magnetic behavior of nanoparticles.[14,15]

In order to clarify the magnetic behavior of FePt $L1_0$ in the nanoscale region avoiding the above experimental difficulties, preparation of perfectly aligned FePt $L1_0$ nanoparticles that are free from any variant domains is essential. Recently, we have reported high-quality FePt $L1_0$ (001) films epitaxially grown on MgO (100) with no variant domains.[3] In this study, we have successfully prepared perfectly aligned single-crystal FePt $L1_0$ (001) nanoparticles by decreasing the nominal film thickness to less than 3 nm. The surface effect of FePt $L1_0$ is explored by coating with different noble metals (Pt and Ag). Since Pt in contact with ferromagnetic material is polarized and thus gives large magnetic interface anisotropy,[16,17] whereas Ag is hardly polarized,[16] it can be expected that these two overlayers give different surface effects.

In the present work, we investigate the magnetic properties of single-crystal FePt $L1_0$ (001) nanoparticles with various sizes and different coating layers. It is revealed that very large magnetic anisotropy of FePt $L1_0$ remains even in the dimension of several atomic layers along the *c* axis, and their magnetic switching is fully described by the coherent rotation model. Moreover, we will point out the significant change of coercivity due to the existence of a Pt overlayer.

II. EXPERIMENTS

FePt was directly deposited on MgO (100) single crystal substrate by dc magnetron sputtering. The substrate temperature T_s and the Ar pressure P_{Ar} during sputtering were fixed, respectively, at 973 K and 10 mTorr, yielding highly ordered

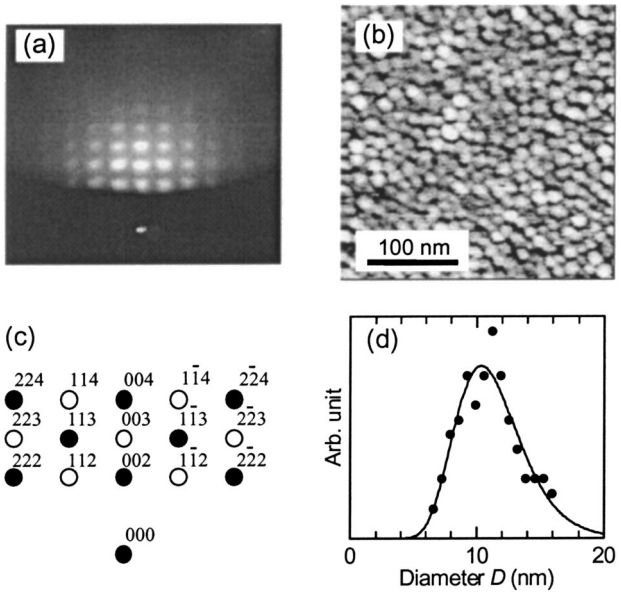

FIG. 1. Representative RHEED pattern taken along MgO [110] (a) and AFM image (b) of FePt particles with nominal deposition thickness d of 1 nm. (c) is an illustration of the diffraction spots of $L1_0$ (001) along [110]. The solid and open circles in (c) indicate the fundamental and superlattice spots from the (hkl) plane. (d) is the particle size distribution of (a). The solid curve in (d) is the best fitting by Eq. (1).

epitaxial FePt $L1_0$ (001) with no variant domains.[3] The nominal deposition thickness d of FePt was varied from 0.5 to 3 nm with the fixed deposition rate of 2.4 nm/min. In such an ultrathin region, FePt nanoparticles are isolated from each other, and their size is well controlled by adjusting the nominal thickness d. Isolation of the particles was confirmed by atomic force microscopy (AFM), transmission electron microscopy (TEM), and electrical resistivity measurements. After cooling the samples to room temperature, a 4-nm-thick Pt or a Ag overlayer was deposited as a coating layer. These overlayers also work as electrodes for the anomalous Hall effect (AHE) measurement. The very high sensitivity of the AHE makes it possible to measure accurately the vertical magnetization component of FePt nanoparticles.[18] The AHE measurements were carried out using a four-probe ac resistance bridge at 980 Hz with a very low bias current of 10 μA. The crystal structure and its orientation were identified by reflection high-energy electron diffraction (RHEED) and x-ray diffractometry (XRD).

III. RESULTS

Figures 1(a) and 1(b) are a representative RHEED pattern and an AFM image of FePt particles with nominal deposition thickness of $d=1$ nm, showing epitaxial growth of nanoscale FePt particles. As depicted in Fig. 1(c), very strong superlattice diffractions, such as 003, 112, and so on, are clearly observed, indicating that the crystal structure of the FePt nanoparticles is highly ordered $L1_0$ (001). The particle size distribution $f(D)$ in Fig. 1(d) can be fitted very well by the following log-normal distribution function (the solid line in the figure):

$$f(D)=\frac{1}{D\sqrt{2\pi\sigma^2}}\exp\left\{-\left[\ln\left(\frac{D}{D_m}\right)\right]^2\frac{1}{2\sigma^2}\right\}, \qquad (1)$$

where D is the particle diameter, D_m is the mean diameter, and σ is the dispersion. The mean particle height h_m was evaluated from the crystalline coherence length of FePt $L1_0$ (001) diffractions that were measured using a very narrow parallel beam through a 1/8° slit.[19] In general, grain boundaries, lattice imperfections, and/or nonuniform strain in a crystal broaden diffraction peaks, resulting in underestimation of the crystal size. However, as verified by the cross-sectional lattice image in Fig. 2, perfect crystalline coherency is confirmed in our samples with very small inclusion of dislocations. One may say that the lattice misfit at the interface of FePt/MgO (misfit ~9%) gives rise to a nonuniform strain distribution along the film normal. However, such a strain distribution due to the lattice misfit is estimated to broaden the FePt $L1_0$ (001) diffraction only by ~5%.[20] Thus the mean particle height h_m determined from the crystalline coherence length is reliable for the present samples. Figure 3 plots D_m and h_m as functions of d. Over the whole thickness range examined in the present study, D_m is proportional to d as $D_m \sim 10d$ and h_m is also proportional as $h_m \sim 2d$ for nominal thickness d up to 2 nm. For $d>2$ nm, h_m tends to be saturated, suggesting coalescence of the particles. Thus the aspect ratio ($=h_m/D_m$) remains to be 1/5 and the particle volume is proportional to d^3 in the range of $d \leqslant 2$ nm.

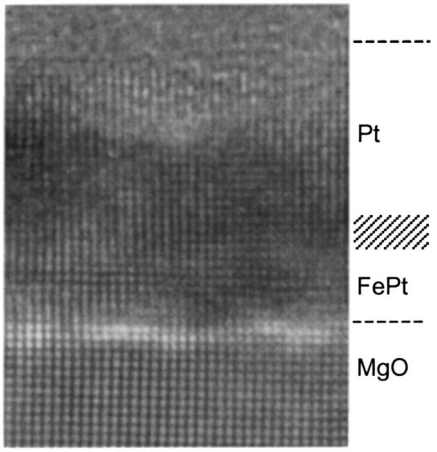

FIG. 2. Cross-sectional lattice image for the 4-nm-thick Pt-coated FePt particles with nominal deposition thickness d of 1 nm.

Figure 4 shows vertical AHE magnetization curves at 10 and 300 K for FePt $L1_0$ (001) particles covered with Pt or Ag overlayer. The shape of all the magnetization curves at low temperature is very similar to that of the two-dimensional assembly of noninteracting particles with vertical magnetic anisotropy.[21] Note in Fig. 4 that the coercivity H_c for the Ag-coated samples with $d>0.5$ nm reaches 70 kOe at 10 K, which is close to the anisotropy field H_k ($=2K_u/M_s$, where K_u is the uniaxial anisotropy constant

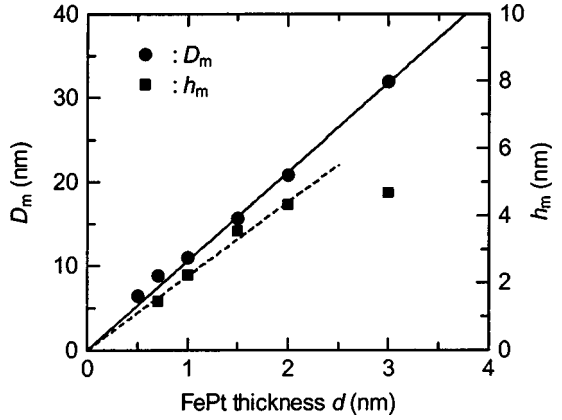

FIG. 3. Mean particle diameter D_m and mean height h_m of FePt particle arrays as a function of the nominal deposition thickness d. Solid and dashed lines indicate the linear fitting of D_m and h_m as guides to the eye.

and M_s is the saturation magnetization) of the highly ordered FePt $L1_0$ single-crystal films.[3] The coercivity monotonically decreases with temperature due to a decrease in K_u and thermal agitation. Compared with Ag overlayers, Pt overlayers give rise to different magnetic behaviors of FePt nanoparticles. The most notable changes are much smaller H_c even at 10 K and a rapid decrease with reduction of the nominal thickness d. In addition, as shown in Fig. 4, the slope of the magnetization curves slightly increases compared with that of Ag-coated samples.

In Figs. 5(a) and 5(b), the coercivity H_c of FePt particles covered with Pt or Ag overlayer is plotted as a function of temperature T. For both kinds of overlayers, H_c decays more rapidly with T as the thickness d decreases. Note that the Ag-coated samples exhibit higher H_c than the Pt-coated ones, and all values of H_c converge to 60–70 kOe at $T=10$ K. This result clearly indicates that magnetic anisotropy K_u as high as bulk FePt $L1_0$ remains even in particles consisting of several atomic layers along the c axis. In contrast, H_c for the Pt-coated samples decreases monotonically with the reduction of thickness d even at 10 K. We measured the angular dependence of the remanent magnetization curves and determined the irreversible switching field H_r as a function of the field direction θ_H with respect to the film

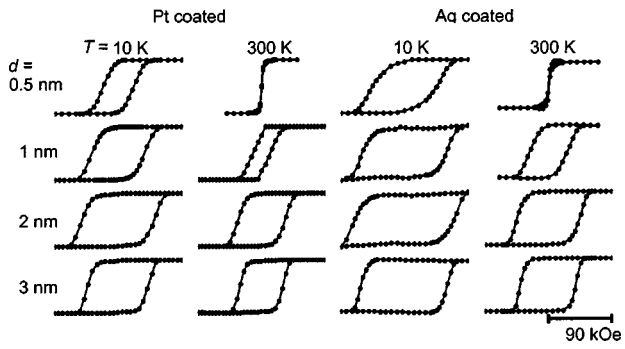

FIG. 4. Magnetization curves obtained by anomalous Hall resistance measurements for the FePt particle arrays covered with Pt and Ag overlayers.

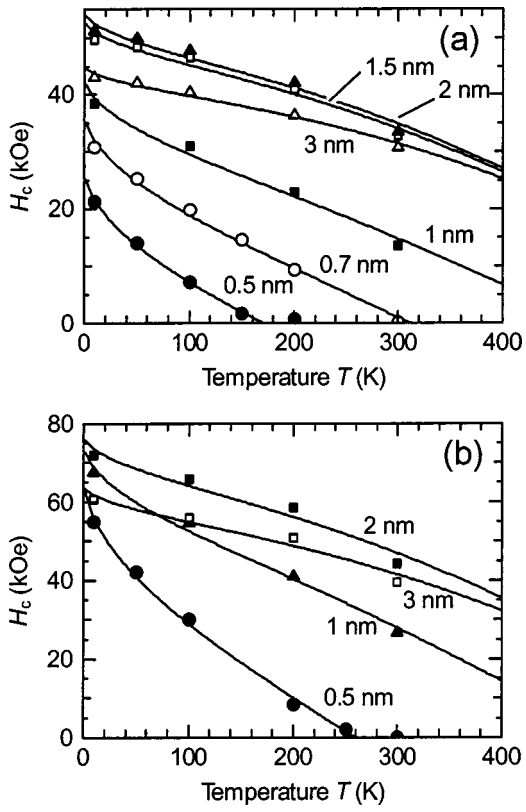

FIG. 5. Temperature-dependent coercivity H_c of FePt particle arrays covered with (a) Pt and (b) Ag overlayers for various nominal deposition thicknesses d. Solid curves are the best fitting by using Eqs. (3)–(6).

normal. Figure 6 shows the angular dependences of $h_r(\theta_H)=H_r(\theta_H)/H_k$ at 10 K for Ag- or Pt-coated FePt $L1_0$ (001) nanoparticles with $d=1$ nm. The dashed line in this figure shows the relation

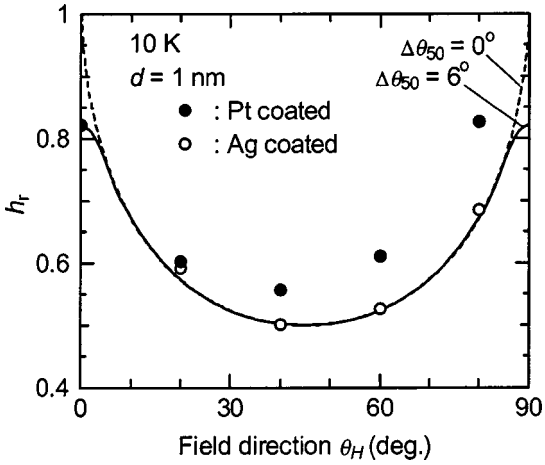

FIG. 6. Angular dependence of the irreversible switching field $h_r(\theta_H)$ of FePt particle arrays with Pt (solid circles) and Ag (open circles) overlayers for nominal deposition thickness $d=1$ nm. Solid and dashed curves indicate the theoretical switching field h_r given by the SW model with and without a c-axis distribution of $\Delta\theta_{50}=6°$, respectively.

$$h_r(\theta_H) = (\cos^{2/3}\theta_H + \sin^{2/3}\theta_H)^{-3/2}, \quad (2)$$

of the Stoner-Wohlfarth (SW) model.[22] Since our epitaxial FePt $L1_0$ (001) particles have a small dispersion of c axis that is evaluated to be $\Delta\theta_{50}=6°$ [full width at half maximum of the (001) rocking curve], probably due to the large misfit at the interface of FePt/MgO. Therefore, $h_r(\theta_H)$ in Eq. (2) is integrated over the solid angle using a Gaussian distribution with c-axis dispersion of $\Delta\theta_{50}=6°$. This c-axis dispersion causes a slight decrease of h_r at around $\theta_H=0°$ and 90° as shown by the solid line in Fig. 6. Here $h_r(0)$ in this figure is adjusted to the calculated value of 0.82. Note that h_r for Ag-coated particles agrees very well with the SW model. This good agreement remains up to the nominal thickness $d=2$ nm, suggesting that each FePt $L1_0$ (001) nanoparticle in the Ag-coated samples behaves as a SW magnet. For $d>2$ nm, however, the angular dependence of h_r tends to deviate from the SW model. On the other hand, h_r for the Pt-coated particles exhibits a slight deviation from the ideal SW model even for $d\leqslant 2$ nm, and then the deviation becomes larger for $d>2$ nm.

Now let us evaluate the anisotropy field H_k and the activation energy E_b of FePt $L1_0$ (001) nanoparticles by analyzing the temperature dependences of H_c presented in Figs. 5(a) and 5(b). Based on the Arrenius-Néel law[23] and SW model, Sharrock[24] and Pfeiffer[25] formulated the temperature dependence of H_c for noninteracting particles under a static reverse field H. However, the usual H_c measurements involve a continuous change of field with time. Therefore, we adopt the following relation rigorously derived by El-Hilo *et al.*,[26] which takes a continuous change of field into account by integrating the reversal probability[27] from $H=0$ to H_c:

$$H_c(T) = \eta H_k(T)\left\{1 - \sqrt{\frac{k_B T}{E_b(T)}\ln\left(\frac{k_B T H_k(T)}{2E_b(T)}\frac{f_0}{R}\right)}\right\}, \quad (3)$$

where k_B is the Boltzmann constant, R is the sweep rate of external field, and $E_b(T)$ is the activation energy for magnetization reversal at zero field, respectively. η is a coefficient determined by the dispersion of easy axis. From the calculation shown in Fig. 6, η is 0.82 for our samples, which have a c-axis dispersion of $\Delta\theta_{50}=6°$. The activation energy E_b can be expressed as

$$E_b(T) = K_u^{\mathrm{eff}}(T) V_m, \quad (4)$$

where V_m is the mean particle volume and $K_u^{\mathrm{eff}}(T)$ is the effective uniaxial anisotropy energy including the demagnetization energy expressed as

$$K_u^{\mathrm{eff}}(T) = K_u(T) - 2\pi N_d M_s(T)^2, \quad (5)$$

where N_d is the demagnetization factor of the particle. The attempt frequency f_0 in Eq. (3) is expressed as[26,27]

$$f_0(T) = \sqrt{\frac{M_s(T)V_m}{2\pi k_B T}}\,\gamma_0 (H_k(T))^{3/2}, \quad (6a)$$

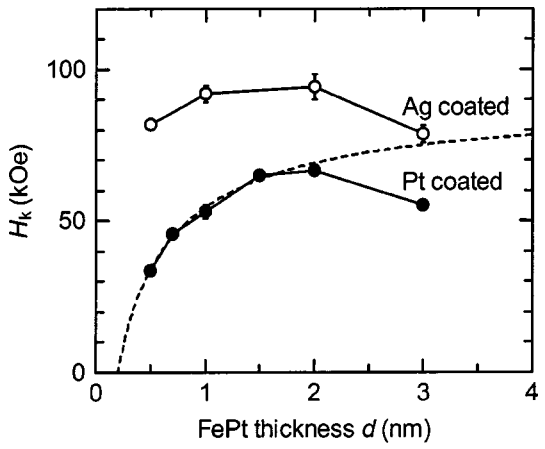

FIG. 7. Replotting of $H_k(0)$ by the best fitting in Figs. 5(a) and 5(b) as a function of the nominal deposition thickness d. Solid and open circles are for the Pt- and Ag-coated FePt particle arrays, respectively. Solid lines are guides to the eye. The dashed line is the calculated anisotropy field H_k assuming $K_u=6.2\times10^7$ erg/cm^3 and $\Delta M=6.6\times10^{-5}$ emu/cm^2.

where γ_0 is the gyromagnetic constant. Using Eq. (4) and $H_k=2K_u^{\mathrm{eff}}/M_s$, Eq. (6a) can be rewritten as

$$f_0(T) = \sqrt{\frac{E_b(T)}{\pi k_B T}}\,\gamma_0 H_k(T). \quad (6b)$$

From Eqs. (3)–(6), we can calculate $H_c(T)$ as a function of temperature if $H_k(T)$ and $E_b(T)$ are known. Since we already know the temperature dependence of M_s and K_u of FePt $L1_0$ single crystal,[3] the data in Fig. 5 can be fitted only by optimizing two parameters $H_k(0)$ and $E_b(0)$. The solid curves in Figs. 5(a) and 5(b) are the best fittings of Eqs. (3)–(6) by adjusting the two parameters. Note that the fittings successfully reproduce the experiments for the whole temperature range. The values of $H_k(0)$ and $E_b(0)$ from the best fitting are plotted in Figs. 7 and 8, respectively. The $H_k(0)$ of the Ag-coated samples is almost constant with

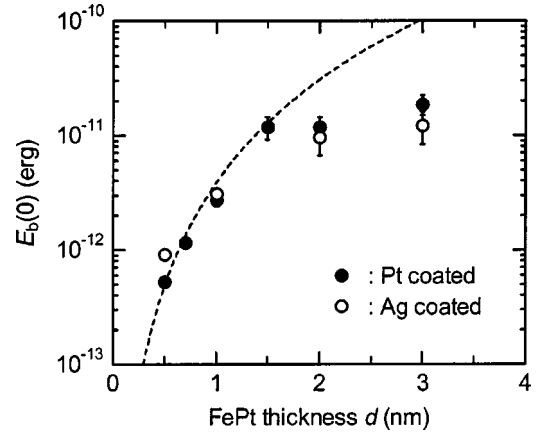

FIG. 8. Replotting of $E_b(0)$ by the best fitting in Figs. 5(a) and 5(b) as a function of the nominal deposition thickness d. Solid and open circles are for the Pt- and Ag-coated FePt particle arrays, respectively. The dashed curve is the best fitting assuming proportionality of $E_b(0)$ with d^3.

about 90 kOe for the nominal thickness $\leqslant 2$ nm, and substituting $M_s(0)=1250$ emu/cm^3 (Ref. 3) into $K_u^{\rm eff}(0)=(1/2)M_s(0)H_k(0)$, $K_u^{\rm eff}(0)$ is evaluated to be $5.6\pm0.5\times10^7$ erg/cm^3. From Eq. (5), the intrinsic anisotropy constant $K_u(0)$ is determined to be $6.2\pm0.5\times10^7$ erg/cm^3. This value of $K_u(0)$ is almost same for the fully ordered FePt $L1_0$ single crystal.[3] In contrast, the Pt-coated samples exhibit smaller $H_k(0)$ and it decreases very rapidly with the decrease of the nominal thickness d. In spite of these different behaviors of $H_k(0)$, $E_b(0)$ is almost the same both for Ag- and Pt-coated samples, and it should be noted that $E_b(0)$ is in proportion to d^3 up to $d<2$ nm, as shown in Fig. 8. The dashed line in the figure is the best fitting of $E_b(0)=3.7\times10^{-12}d^3$ erg/nm^3 in the range of $d<2$ nm. Since the volume V_m of the FePt particle is proportional to d^3 as mentioned before, the above relation is reasonable. The validity of the relation given by the fitting in Fig. 8 can be confirmed as follows. Under the approximation of the particle shape to be a half oblate spheroid, V_m can be evaluated as $V_m\sim\frac{1}{2}(4\pi/3)(D_m/2)^2h_m\sim(100/3)\pi d^3$ using the relations of $D_m\sim10d$ and $h_m\sim2d$ in Fig. 3. Substituting this V_m and $K_u^{\rm eff}=5.6\times10^7$ erg/cm^3 into Eq. (4), we obtain $E_b(0)=K_u^{\rm eff}(0)V_m\sim5.9\times10^{-12}d^3$ erg/nm^3. This estimation of $E_b(0)$ is in fairly good agreement with the best fitting in Fig. 8.

IV. DISCUSSION

The magnetic anisotropy of FePt $L1_0$ (001) nanoparticles is as high as the fully ordered single crystal and is invariant even in the dimension of several atomic layers along the c axis. All the magnetic behaviors of the Ag-coated FePt $L1_0$ (001) nanoparticles with $d<2$ nm can be completely described with the SW model, as confirmed by the angular dependence of H_r in Fig. 6 and coercivity analysis in Fig. 5 by Eqs. (3)–(6) derived from the SW model. For $d\geqslant2$ nm, however, we note in Figs. 7 and 8 that $H_k(0)$ decreases and $E_b(0)$ saturates, probably due to change of the magnetization reversal mode at $d\sim2$ nm ($D_m\sim20$ nm). This is also suggested by the slight deviation of h_r from the SW model for $d>2$ nm as mentioned before. According to the micromagnetic theory by Aharoni,[28] the magnetization reversal mode changes from coherent to incoherent rotation (curling) when the particle diameter D_m exceeds the critical diameter D_c given by

$$D_c=\frac{2q}{M_s}\sqrt{\frac{2A}{N_x}}, \tag{7}$$

where q is the geometrical factor ranging from 2.0816 for a sphere to 2.115 for an infinite sheet,[28] A is the exchange stiffness constant, and N_x is the demagnetizing factor along the long axis of an oblate spheroid. Substitution of $M_s=1250$ emu/cm^3 and $A=1\times10^{-6}$ erg/cm (Ref. 3) into Eq. (8) gives $D_c\sim38$ nm, which is comparable to $D_m\sim20$ nm at $d=2$ nm in Fig. 2.

For the Pt-coated samples, some of different magnetic behaviors compared with the Ag-coated ones are observed. A most notable change is that, as seen in Fig. 5, H_c is always smaller than that for the Ag-coated samples and decreases monotonically with the reduction of the nominal thickness d. The evaluated $H_k(0)$ in Fig. 7 also exhibits the same manner. One may say the effective anisotropy is decreased due to presence of the interface anisotropy at the FePt/Pt interface. In order to explain the reduction of $H_k(0)$, however, we have to assume an extremely large interface anisotropy of 2–3 erg/cm^2, which is one order of magnitude higher than that commonly observed in (Fe, Co)/Pt multilayers.[29–31] Further, the sign of the interface anisotropy in this case should be negative, which is also contrary to the positive interface anisotropy for (Fe, Co)/Pt multilayers. It should be recalled here that the activation energy $E_b(0)=K_u^{\rm eff}(0)\ V_m$ is almost the same for both Ag- and Pt-coated samples as seen in Fig. 8, indicating that $K_u^{\rm eff}(0)$ is essentially independent of the overlayer material. Therefore, we conclude that the interface anisotropy is negligible in our samples. Here we pay attention to the possibility that Pt atoms in contact with FePt are ferromagnetically polarized due to the proximity effect,[32,33] giving rise to an enhancement of the effective magnetic moment. Thus the effective moment $M_s^{\rm eff}$ is

$$M_s^{\rm eff}V_m=M_sV_m+\Delta M\ \ S_m, \tag{8}$$

where ΔM is the induced moment per unit interface area and S_m is the mean interface area. From Fig. 3, we assume the FePt particle shape to be an oblate spheroid with aspect ratio of 1/5. Using the value of $K_u(0)=6.2\times10^7$ erg/cm^3, the thickness dependence of $H_k(0)$ is perfectly reproduced by assuming $\Delta M=6.6\times10^{-5}$ emu/cm^2 at 0 K, as depicted by the dashed line in Fig. 7. This good agreement implies that the induced Pt moment is the main reason for the significant reduction of $H_k(0)$, and $K_u(0)$ is unchanged in the Pt-coated samples. It is reported that the induced moment of Pt in contact with Fe is $0.5\mu_B$/atom and nearly constant with Pt thickness up to 1 nm,[33] giving $\Delta M\geqslant3\times10^{-5}$ emu/cm^2 at 300 K. Moreover, the same order of induced moment has been observed in Pd/Co ($\sim2\times10^{-5}$ emu/cm^2 at 300 K) (Refs. 34–36) and Pd/NiO multilayer ($\sim1\times10^{-4}$ emu/cm^2 at 4.2 K) (Ref. 37). Even though our assumption of $\Delta M=6.6\times10^{-5}$ emu/cm^2 at 0 K is reasonable in comparison with the values previously reported, contradicted results have been also reported that the induced moment of Pt on Fe or Co decays exponentially within a very small Pt thickness range of 1 nm,[38–40] giving a much smaller ΔM. We have to point out the possibility that $H_k(0)$ for the Pt-coated samples in Fig. 8 is somewhat underestimated due to a slight deviation of the switching behavior from the ideal SW model. This is seen in the little deviation of the angular dependence of h_r from the SW model as seen in Fig. 6 and the larger slope of the vertical magnetization curves as in Fig. 4. These results would be attributed to a weak exchange coupling between neighboring FePt nanoparticles through polarized Pt atoms near the Pt/FePt interface. In fact, several micromagnetic and analytical calculations suggest similar features due to weak exchange coupling between grains.[21,41,42] However, the validity of our coercivity analysis by Eqs. (3)–(6) for the Pt-coated samples was checked by modifying H_k in Eq. (3) and very little change of $E_b(0)$ was confirmed. Thus, although it

is likely that $H_k(0)$ is somewhat underestimated due to a weak exchange coupling between FePt nanoparticles, the above discussions remain essentially unchanged.

V. CONCLUSION

We have prepared single-crystal FePt $L1_0$ (001) nanoparticles grown on MgO (100). The particles have the shape of thin oblate spheroids with aspect ratio (height/diameter) of about 1/5 and the mean diameter D_m ranging from 5 to 30 nm. FePt $L1_0$ nanoparticles exhibit an extremely large coercivity of 70 kOe at 10 K, which is close to the anisotropy field of the highly ordered FePt $L1_0$. This is a good evidence that the very high magnetic anisotropy of FePt remains even in the dimension of several atomic layers along the *c* axis of the $L1_0$ phase. All the magnetic properties, such as the angular dependence of the irreversible switching field, the magnitude of H_c, and the activation energy for the magnetization reversal, for the Ag-coated FePt nanoparticles with $D_m < 20$ nm can be fully described by the coherent rotation model, while for $D_m \geqslant 20$ nm the magnetic behaviors deviate from the coherent rotation model, indicating a change of the magnetization reversal mode from coherent to incoherent rotation. For the Pt-coated samples, in spite of little deviation from the ideal SW model, the magnetic behaviors for $d < 2$ nm can be also understood within the framework of the SW model by taking Pt polarization into account. The most notable effect of Pt coating is an appreciable reduction of the coercivity of FePt particles, although the activation energy of magnetization reversals remains unchanged. These results suggest that enhancement of the effective magnetic moment due to Pt polarization at the Pt/FePt interface reduces the effective anisotropy field, while the magnetic anisotropy is unchanged.

ACKNOWLEDGMENTS

The present work has been supported by Industrial Technology Research Grant Program in 02 from NEDO of Japan, the Grant-in-Aid of the Japan Society for the Promotion of Science, 21st Information Center at Tohoku University, and the Storage Research Consortium in Japan. The authors wish to express gratitude to Dr. K. Hono at NIMS for TEM observations, and Y. T. acknowledges support of the Japan Society for the Promotion of Science.

*Corresponding author. Electronic address: okamoto@tagen.tohoku.ac.jp

[1] D. Weller, A. Moser, L. Folks, M. E. Best, L. Wen, M. F. Toney, M. Schwickert, J.-U. Thiele, and M. F. Doener, IEEE Trans. Magn. **36**, 10 (2001).
[2] H. Kanazawa, G. Lauhoff, and T. Suzuki, J. Appl. Phys. **87**, 6143 (2000).
[3] S. Okamoto, N. Kikuchi, O. Kitakami, T. Miyazaki, Y. Shimada, and K. Fukamichi, Phys. Rev. B **66**, 024413 (2002).
[4] O. Kitakami, N. Kikuchi, S. Okamoto, Y. Shimada, K. Oikawa, Y. Otani, and K. Fukamichi, J. Magn. Magn. Mater. **202**, 305 (1999).
[5] N. Inaba, Y. Uesaka, and M. Futamoto, IEEE Trans. Magn. **36**, 54 (2000).
[6] M. L. Yan, H. Zeng, N. Powers, and D. J. Sellmyer, J. Appl. Phys. **91**, 8471 (2002).
[7] T. Saito, O. Kitakami, and Y. Shimada, J. Magn. Magn. Mater. **239**, 310 (2002).
[8] H. Sakaue, T. Miyazaki, O. Kitakami, and Y. Shimada, J. Magn. Soc. Jpn. **25**, 847 (2001).
[9] S. Sun, C. B. Murray, D. Weller, L. Folks, and A. Moser, Science **287**, 1989 (2000).
[10] B. Bian, K. Sato, Y. Hirotsu, and A. Makino, Appl. Phys. Lett. **75**, 3686 (1999).
[11] G. H. O. Daalderop, P. J. Kelly, and M. F. H. Schuurmans, Phys. Rev. B **44**, 12 054 (1991).
[12] A. Sakuma, J. Phys. Soc. Jpn. **63**, 3054 (1994).
[13] L. Szunyogh, P. Weinberger, and C. Sommers, Phys. Rev. B **60**, 11 910 (1999).
[14] C. Chen, O. Kitakami, and Y. Shimada, J. Appl. Phys. **84**, 2184 (1998); C. Chen, O. Kitakami, S. Okamoto, and Y. Shimada, *ibid.* **86**, 2161 (1999).
[15] M. Jamet, M. Négrier, V. Dupuis, J.-T Combes, P. Mélinon, A. Pérez, W. Wernsdorfer, B. Barbara, and B. Baguenard, J. Magn. Magn. Mater. **237**, 239 (2001).
[16] H. Ebert, S. Ruegg, G. Schütz, R. Wienke, and W. B. Zepper, J. Magn. Magn. Mater. **93**, 601 (1991).
[17] K. Kyuno, R. Yamamoto, and S. Asano, J. Phys. Soc. Jpn. **61**, 2099 (1992).
[18] A. Gerber, A. Milner, J. Tuaillon-Combes, M. Négrier, O. Boisron, P. Mélinon, and A. Perez, J. Magn. Magn. Mater. **241**, 340 (2002).
[19] B. D. Culity, *Elements of X-ray Diffraction* (Addison-Wesley, Reading, MA, 1956).
[20] We assumed that the strain due to lattice misfit at the FePt/MgO interface linearly decreases to zero at the FePt surface. This assumption is a maximum strain distribution, giving maximum diffraction broadening.
[21] J.-G. Zhu and N. H. Bertram, J. Appl. Phys. **66**, 1291 (1989).
[22] E. C. Stoner and E. P. Wohlfarth, Philos. Trans. R. Soc. London, Ser. A **240**, 599 (1948).
[23] L. Néel, Adv. Phys. **4**, 191 (1955).
[24] M. P. Sharrock, IEEE Trans. Magn. **26**, 193 (1990).
[25] H. Pfeiffer, Phys. Status Solidi A **118**, 295 (1990).
[26] M. El-Hilo, A. M. de Witte, K. O'Grady, and R. W. Chantrell, J. Magn. Magn. Mater. **117**, L307 (1992).
[27] W. F. Brown, J. Appl. Phys. **30**, 130S (1959); **34**, 1319 (1963).
[28] A. Aharoni, J. Appl. Phys. **30**, 70S (1959); Phys. Status Solidi **16**, 1 (1966).
[29] C.-J. Lin, G. L. Gorman, C. H. Lee, R. F. C. Farrow, E. E. Marinero, H. V. Do, H. Notarys, and C. J. Chien, J. Magn. Magn. Mater. **93**, 194 (1991).
[30] M. T. Johnson, R. Jungblut, P. J. Kelly, and F. J. A. den Broeder, J. Magn. Magn. Mater. **148**, 118 (1995).
[31] T. Katayama, Y. Suzuki, Y. Nishihara, T. Sugimoto, and M. Hashimoto, J. Appl. Phys. **69**, 5658 (1991).
[32] J. L. Pérez-Díaz and M. C. Muñoz, J. Appl. Phys. **75**, 6470 (1994).
[33] W. J. Antel, Jr., M. M. Schwickert, T. Lin, W. L. O'Brien, and G. R. Harp, Phys. Rev. B **60**, 12 933 (1999).
[34] B. N. Engel, C. D. England, R. A. Van Leeuwen, M. H. Wied-

mann, and C. M. Falco, Phys. Rev. Lett. **67**, 1910 (1991).
[35] R. H. Victra and J. M. MacLaren, Phys. Rev. B **47**, 11 583 (1993).
[36] S. Okamoto, K. Nishiyama, O. Kitakami, and Y. Shimada, J. Appl. Phys. **90**, 4085 (2001).
[37] T. Manago, T. Ono, H. Miyajima, K. Kawaguchi, and M. Sohma, J. Phys. Soc. Jpn. **68**, 334 (1999).
[38] R. Bertacco and F. Ciccacci, Phys. Rev. B **57**, 96 (1998).
[39] S. Ferrer, J. Alvarez, E. Lundgren, X. Torrelles, P. Fajardo, and F. Boscherini, Phys. Rev. B **56**, 9848 (1997).
[40] J. Geissler, E. Goering, M. Justen, F. Weigand, G. Schutz, J. Langer, D. Schmitz, H. Maletta, and R. Mattheis, Phys. Rev. B **65**, 020405 (2001).
[41] O. Kitakami and Y. Shimada, Jpn. J. Appl. Phys., Part 1 **40**, 4019 (2001).
[42] W. Chen, S. Zhang, and H. N. Bertram, J. Appl. Phys. **71**, 5579 (1992).